K-Isomers in Very Neutron-Rich Nuclei Around Mass 180

C. Schlegel[1*], P.H. Regan[2], M. Pfützner[3], J. Gerl[1], M. Hellström[4], Zs. Podolyák[2], M. Caamaño[2], P. Mayet[1], A. Aprahamian[2], J. Benlliure[5], A.M. Bruce[6], P.A. Butler[7], D. Cortina Gil[1], D.M. Cullen[7], J. Döring[1], T. Enquist[1], F. Farget[8], C. Fox[7], J. Garcés Narro[2], W. Gelletly[2], J. Giovinazzo[9], M. Górska[1], H. Grawe[1], R. Grzywacz[10], A. Kleinböhl[1], W. Korten[11], M. Lewitowicz[12], R. Lucas[11], H. Mach[14], M. Mineva[4], C. O'Leary[7], F. De Oliveira[12], C.J. Pearson[2], M. Rejmund[8], M. Sawicka[3], H. Schaffner[1], K. Schmidt[1], Ch. Theisen[11], P.M. Walker[2], D.D. Warner[13], C. Wheldon[2], H.J. Wollersheim[1], S. Wooding[12], F. Xu[2]

[1]GSI, Planckstrasse 1, D-64291 Darmstadt, Germany
[2]Dept. of Physics, University of Surrey, Guildford, GU2 5XH, UK
[3]Institute of Experimental Physics, Warsaw University, Pl-00861 Warsaw, Poland
[4]Div. of Cosmic and Subatomic Physics, Lund University, SE-22100, Sweden
[5]Dept. Física de Partículas, University of Santiago de Compostela, Spain
[6]Dept. of Mathematical Science, University of Brighton, Brighton BN2 4GJ, UK
[7]Dept. of Physics, University of Liverpool, Liverpool, L69 3BX, UK
[8]IPN, 91406 Orsay Cedex, France
[9]CNRS Bordeaux, France
[10]University of Tennesse, Knoxville 37996, USA
[11]CEA Saclay, Paris, France
[12]GANIL, BP 5027, F-14021 Caen Cedex, France
[13]Daresbury Laboratory, Warrington, WA4 4AD, UK
[14]Dept. of Neutron Research, Uppsala University, S-61182 Nyköping, Sweden

*e-mail: C.Schlegel@gsi.de

Abstract

γ-spectroscopy methods have been used to search for microsecond isomers among the fragmentation products of a 1 GeV/nucleon ^{208}Pb beam. In particular the population of the of the known $K^{\pi}=35/2^{-}$ isomer in ^{179}W has been investigated and several new isomeric decays have been found for neutron rich nuclei in the A$\approx$180-200 mass region. The ground state band of the neutron rich N=116 system of ^{190}W has been identified for the first time and we discuss its structure in comparism to neighboring systems.

1. Introduction

Isomeric states formed by the de-coupling of multiple pairs of nucleons in deformed nuclei are predominantly found in the A$\approx$180 region of the nuclear chart. By coupling high angular momenta of unpaired nucleons together, states with high values of the K quantum number can be formed. Decays of these states to states with lower K values are hindered. The high-K configurations are therefore often isomeric with half-lifes ranging from nanoseconds to years. The most spectacular examples are predicted for the neutron

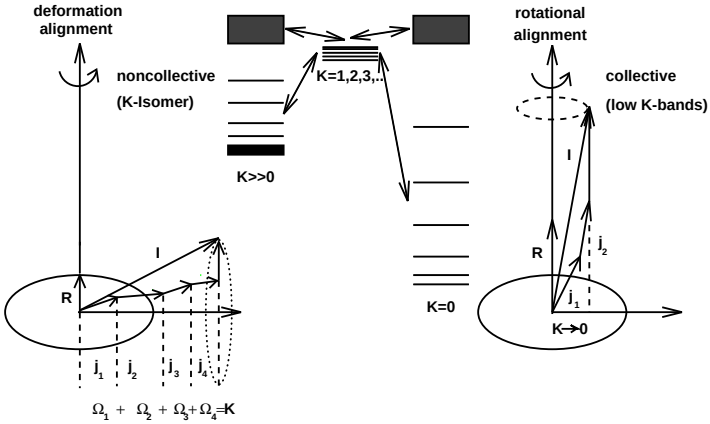

Figure 1: Change from deformation aligned single particle spins to rotation aligned spins.

rich side of the valley of stability and are thus not reachable by standard nuclear reactions [1].

The projection, K, of the total angular momentum on the symmetry axis of axially-symmetric deformed nuclei approximates to a good quantum number. This leads to the electromagnetic selection rule for the decay of a nuclear state: $\Delta K \leq \lambda$, where λ is the transition multipolarity. Nevertheless, recent studies in the Hf, Ta, W and Os isotopes show highly K-forbidden transitions [2, 3, 4] where the degree of K-forbiddeness given by: $\nu = \Delta K - \lambda$, ranges from low values up to 24 for ^{182}Os.

Suggestions for the mechanisms to explain such highly forbidden transitions include Coriolis mixing, (see Fig.1), of different K-values as well as tunneling through a potential barrier between the ground state (gs) and a second potential minimum caused by a triaxial shape (γ-degree of freedom) as shown in Fig.2.

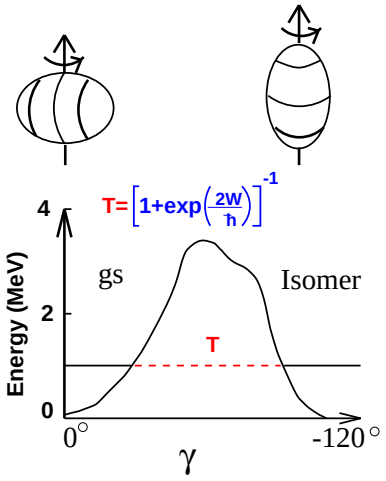

Figure 2: Schematic, showing a cut through the potential energy surface in γ-direction shows the barrier between K-isomer and gs.

In the first case the Coriolis interaction mixes the wave functions of deformation aligned (K isomers) and rotational aligned configuration (gs-band) and hence enables these forbidden transitions.
The other approach involves shape fluctuations where the orientation of the nucleus changes from prolate shape (γ=-120°) with noncollective rotation to prolate shape with collective rotation (γ=0°) through the intermediate oblate γ=-60°configuration. The transmission probability is given by the energy potential barrier which separates both configurations.
Open questions concerning the research of K-isomers in this region include:

- What is the behaviour of K-isomers on the neutron rich side of the valley of stability? There are predictions of very long lived isomers [1], like the 16^+-Isomer in ^{178}Hf ($T_{1/2}$=31y).
- What can we learn about the shell structure of unstable neutron rich nuclei? K-isomers provide access to nearly pure multi quasiparticle states.
- Many K-isomers are involved in the s- and r-nucleosynthesis processes. Interaction with the hot photon bath present in the astrophysical sites may lead to depopulation of the isomers, drastically altering their effective half-lives.
- To what extent does K remain a a good quantum number at higher excitation energies and angular momenta?
- Where are the limits of K-forbiddeness? How far from the yrast line are the K-isomers situated? Is there statistical K-mixing at higher level density?
- What is the influence of the pairing interaction in the population process of multi quasiparticle K-isomers?

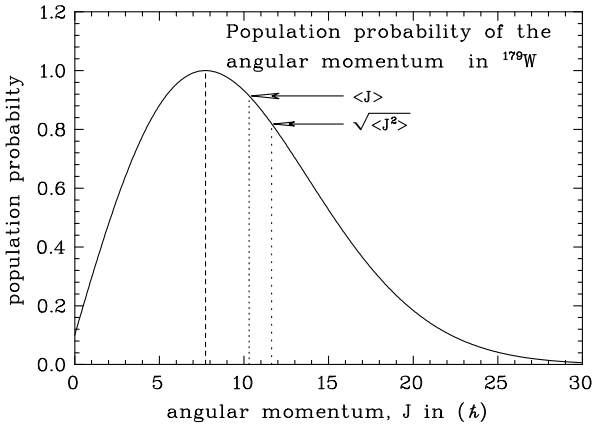

Figure 3: Distribution of the angular momentum which can be populated in a fragmentation process for the case of ^{179}W (using the prescription outlined in [6]).

Another important aspect concerning the production of isomers with radioactive ion beams is the angular momentum dependence of the population probability of K-isomers in the projectile fragmentation process. Prior to the current work, were no information on measured isomeric ratios in the A≈180 region. The isomeric ratio is defined as the ratio between the production yield of the isomeric state and the total production of that isotope. One can estimate the angular momentum distribution of the final fragments in the framework of the abrasion-ablation model [6]. In this model, the population of a fragment with a well determined angular momentum is a purely statistical process. As an example (Fig. 3) the distribution of angular momenta which can be populated in the

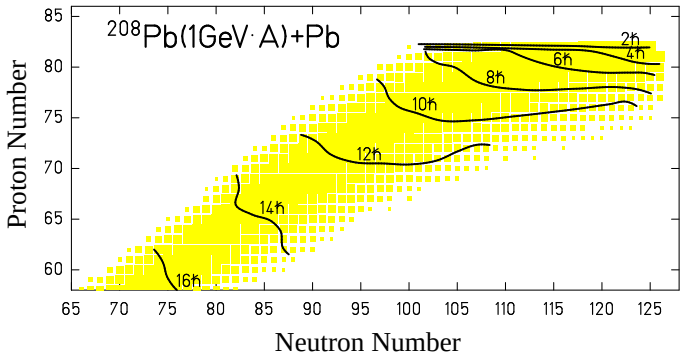

Figure 4: The r.m.s. angular momenta of the final fragments calculated for the reaction at 1·GeV· A ^{208}Pb + a ^{208}Pb. The squares indicate the relative yields of the corresponding isotopes on a logarithmic scale. The figure is taken from [6].

fragmentation process of a Pb-beam on a Be-target is calculated for the case of ^{179}W. The calculations are done using an approximate formula outlined in [6]. The picture shows that beyond the r.m.s value of the angular momentum of $\sqrt{< J^2 >} \approx 10\hbar$ higher angular momenta up to $30\hbar$ are also possible. Figure 4 shows the calculation of the r.m.s value of the angular momentum as a function of the neutron- and proton number for the fragmentation of a Pb-beam on a Pb-target. One should note that in the present experiment we used a Pb-beam on a Be-target.

2. Experimental Technique

To select neutron rich ions in the mass 180-200 region we performed our experiment using the GSI-Fragment-Separator (FRS) [9]. The gamma radiation emitted from the implanted exotic isotopes was measured with a Segmented Clover array. This is an extension of the setup used by Pfützner et al. to study isomers in neutron rich Pb isotopes following the fragmentation of a ^{238}U beam [10]. The arrangement of the experimental set up is shown in Fig. 5. The FRS, which is a magnetic zero-degree spectrometer consisting of 2

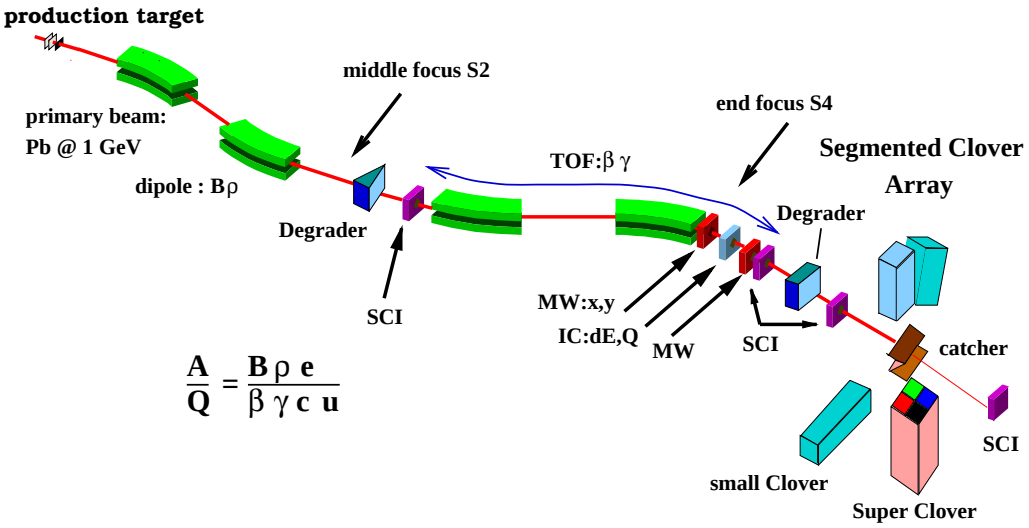

Figure 5: Schematic picture of the FRS and the experimental setup.

dipole stages, was operated in the achromatic mode. The ions of interest were produced in fragmentation of a 1 GeV per nucleon lead beam from the GSI heavy-ion synchrotron SIS on a 1.6 g/ cm^2 beryllium target.
The principle of separation and identification are the following [7, 9]:

-The first dipole stage selects fragments according to their momentum-to-charge ratio. Since all fragments have nearly the same velocity, this corresponds to a separation according to mass-to-charge ratio, A/Q. Charge identification is done by plotting A/Q versus x-position at the intermediate focal plane S2, see Fig. 6. In this Figure, the three

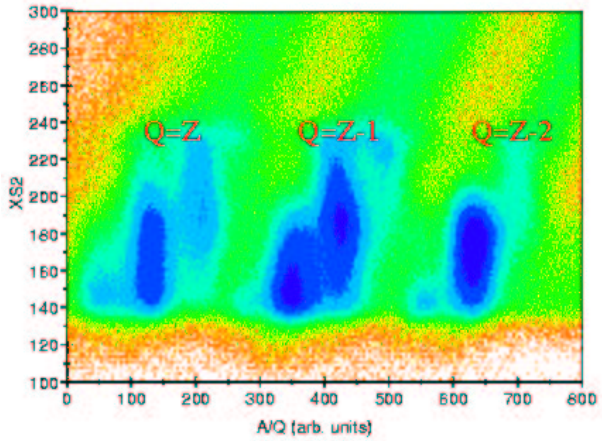

Figure 6: Charge selection for the ^{191}W setting. The three main groups correspond to different charge states, see the text. The structure inside each group corresponds to different Z values.

main groups of events represent ions that i) did not change charge state, ii) picked up one electron and iii) picked up two electrons during the passage through materials at S2. The leftmost group predominantly contains ions that were fully stripped.

-A second selection is achieved by introducing a wedge-shaped aluminum degrader at S2. The thickness was chosen to be $\approx 50\%$ of the range of the selected fragments. The energy loss in the degrader mainly depends on the atomic number Z and velocity (expressed by the relativistic parameters β and γ, see also Fig. 5) of the fragment and the various ion species are therefore spatially separated in the second dipole stage. Thus, individual nu-

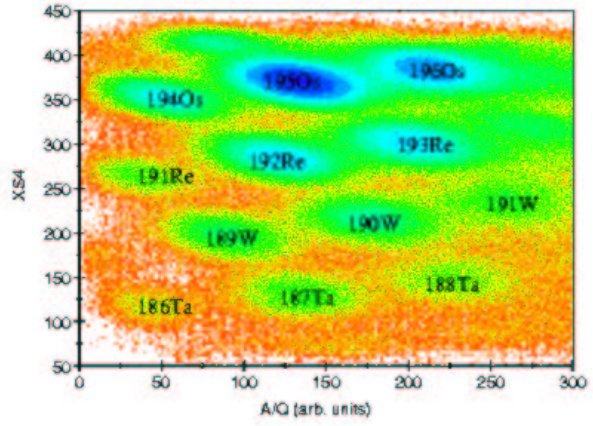

Figure 7: Isotope identification plot for the 191W setting. Only ions that did not change charge state at S2 (predominantly fully stripped) are shown.

clides can be selected in a plot of position at the final focus S4 versus A/Q *after selecting the appropriate charge state group*, see Fig. 7.

After reaching the focal plane of the FRS, the ions were slowed down in a thick aluminum degrader prior to being implanted into a catcher foil. To identify and suppress events resulting from secondary breakup reactions, a scintillator was placed between the degrader and the catcher. A second scintillator placed after the catcher served as a veto counter. Surrounding the catcher, an array consisting of four segmented Clover detectors was mounted, see Fig.8. The absolute photopeak efficiency of the Segmented Clover array was measured to be about 6% at 1.3 MeV and about 17% at 300 keV. The efficiency was determined for different catcher-positions to obtain a position dependent absolute photopeak efficiency, which is necessary for the correct determination of the absolute isomeric ratios. Fig. 8 shows the mechanical arrangement of the four Segmented Clover detectors. The GSI-Super Clover was mounted with an active BGO shield to suppress break-up events and to have the possibility to reduce Compton background. The delay of gamma-rays (with respect to the implantation time of the corresponding heavy ion) was

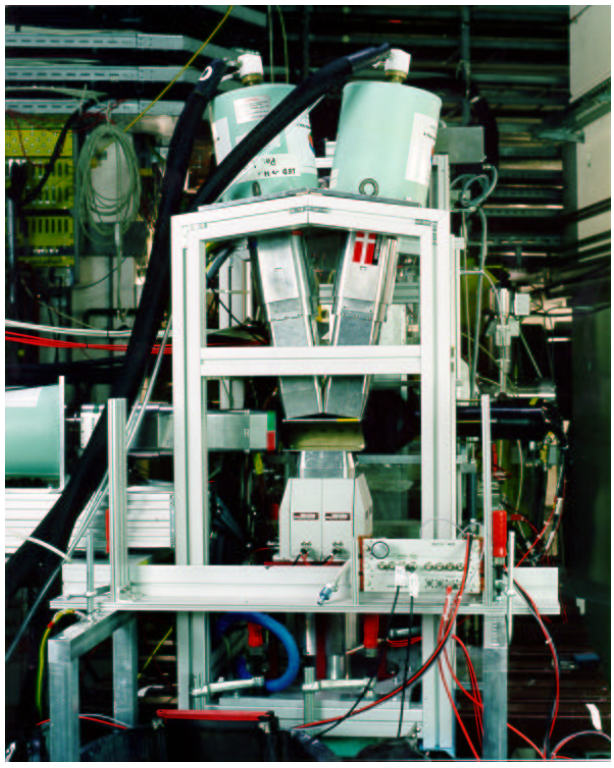

Figure 8: Photograph of the Gamma-array including the GSI-Super-Clover and 3 standard Clovers from France and UK. In addition the Super-Clover was surrounded by an active BGO-anti Compton shield. All the clover detectors are 4 fold segmented and have an energy resolution of $\approx$ 2.5 keV. The absolute efficiency of the Clover array was around 6% at 1.33 MeV for the central position of the catcher.

measured in two time ranges: 8 μs (TDC) and 80 μs (TAC). In addition, a long-range counter covered the entire spill length (up to 8 seconds) was used. All events for a specific isotope were accumulated in time-energy-matrices in order to determine times for different γ-transitions. In the γ-ray spectra the prompt events within the first 550 ns were rejected.

3. First Results

To investigate the population of K isomers in the A≈180-200 region using fragmentation reactions, decays in nuclei in the valley of stability were selected first. One example for the population of a high-spin state is the known $K^\pi=35/2^-$ isomer with a half-life of 750 ns in ^{179}W previously measured by Walker et al. [11]. In the spectrum (Fig.9) gamma transitions of the gs-band are seen up to the transition $31/2^- \rightarrow 27/2^-$. All observed gamma ray lines are shown in the partial level scheme in Fig. 10. The feeding transition from the $K^\pi=35/2^-$ isomer into the $K^\pi=31/2^-$ state of the gs-band was observed at 610 keV. Beside this isomer another state with $K^\pi=21/2^+$ and a half-life of 390 ns was populated. In contrast to the $K^\pi=35/2^-$ isomer this state decays first to the $K^\pi=9/2^+$ side band and then to the gs-band. The intensity of the γ-ray lines seen in the spectrum originating from the decay of the $K^\pi=21/2^+$ isomer are less due to the shorter

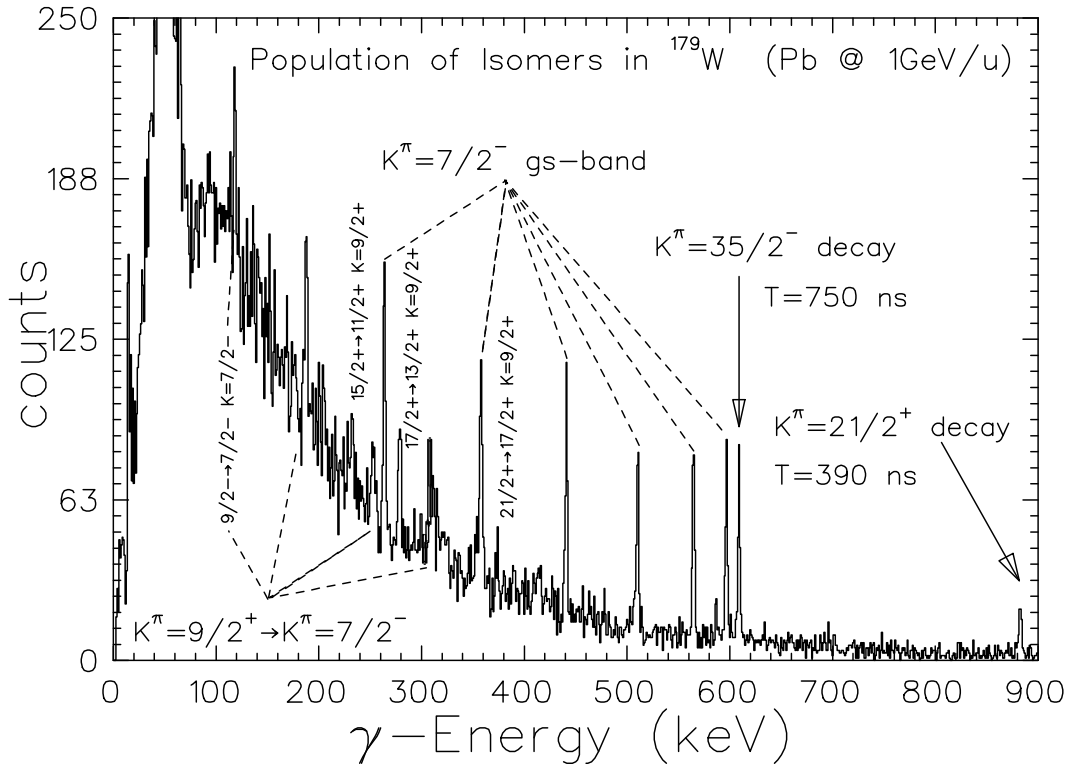

Figure 9: Gamma-ray spectrum of ^{179}W.

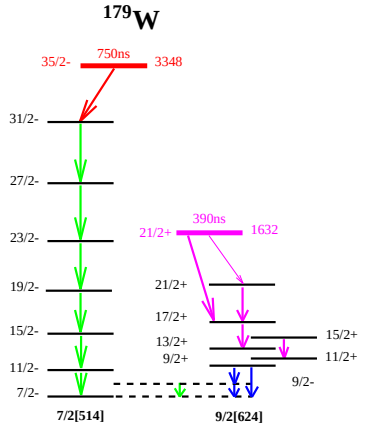

Figure 10: Partial level Scheme of ^{179}W taken from [11].

half-life compared to the $K^{\pi}=31/2^{-}$ state. This is because the time window used in this analysis begins about 850ns after the fragmentation reaction. This corresponds, in case of the $K^{\pi}=35/2^{-}$ isomer to one half-life while for the $K^{\pi}=21/2^{+}$ isomer it is two half-lifes. The decay from this isomer to the $I^{\pi}=17/2^{+}$ state of the $K^{\pi}=9/2^{+}$ band is clearly seen in the spectrum at 884 keV. The $K^{\pi}=9/2^{+}$ band decays with a half-life of 1.6 ns to the gs-band. Due to this feeding one can observe the $9/2^{-} \rightarrow 7/2^{-}$ transition in the gs-band at 119 keV.
Figure 11 shows the excitation energy as a function of the angular momentum of ^{179}W with known K-isomers taken from [11]. The gs-band collective states are given up to spin $47/2\ \hbar$. It should be noted that in the current experiment the gs-band was only observed

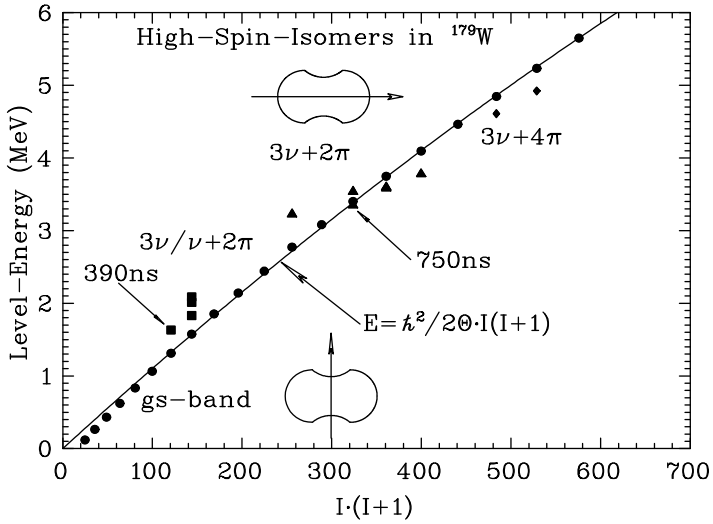

Figure 11: Ground state rotational band and known K-isomers in ^{179}W [11].

up to the $35/2^-$-state since the population of a long enough lived isomeric state was required. The solid line shows a fit using the rigid rotor formula including the high spin levels. In addition all known quasiparticle isomers are shown. Transitions from isomers marked by arrows were observed in the experiment. The other isomers have half-lifes which are outside the time range of the experiment.
From the distribution shown in Fig. 3, a population probability for a spin of $10\hbar$ and $17\hbar$ is given by 0.93 and 0.36, respectively. This results in a ratio of $\approx$0.4 for the population of the $K^\pi=35/2^-$ relative to the $K^\pi=21/2^+$ isomer. By contrast, in the experiment, we obtain a ratio of 0.7, which indicates that the $K^\pi=35/2^-$ isomer was more stronger populated than expected. One explanation maybe the yrast location of the $K^\pi=35/2^-$ state. It therefore acts as an yrast trap which is strongly fed from states with higher spin. The $K^\pi=21/2^+$ state in contrast to the $K^\pi=35/2^-$ isomer lies above the yrast line and is not fed so significantly by higher spin states.
In several exotic settings of the FRS a number of new isotopes in the mass 180-200 region were discovered. The spectroscopy of γ-transitions from the decay of the K-isomers proves to be a novel method to access the structure of excited medium and high spin states in neutron rich unstable nuclei which are not reachable by other types of reaction. As an example the population of the previously unknown gs-band in ^{190}W is shown in Fig.12. A simple analysis of the gs-band using the Harris parametrisation [12] cannot reproduce the proposed level ordering. ^{190}W seems to be not a prolate rotor like ^{182}W but rather

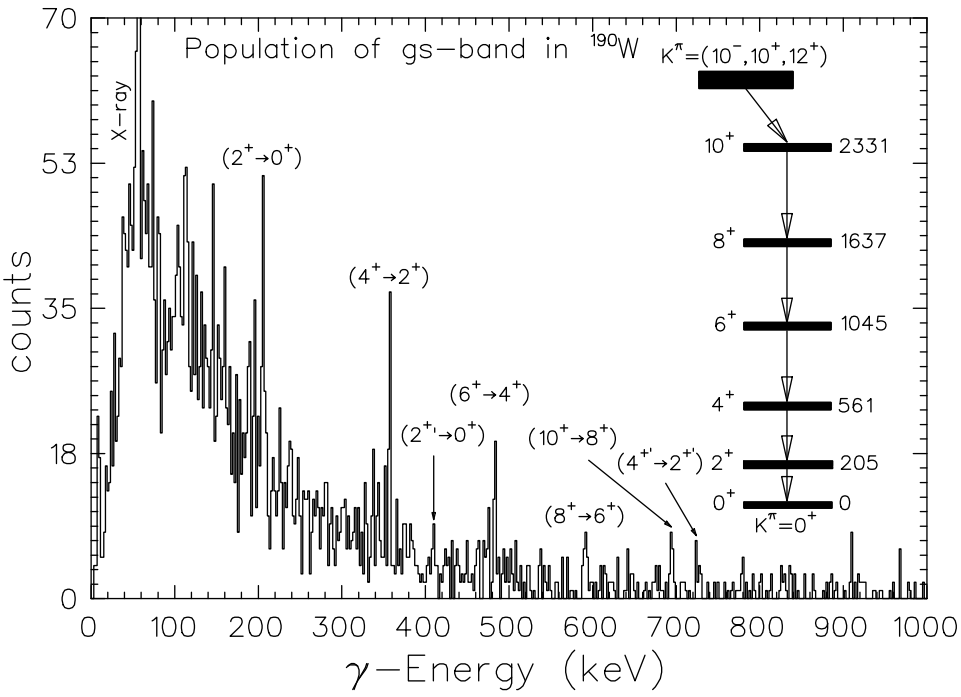

Figure 12: Gamma-ray spectra of ^{190}W.

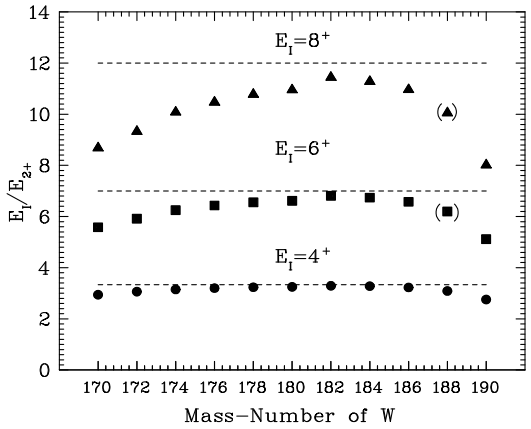

Figure 13: Level-energies of the W isotopes normalized to the 2^+ gs level.

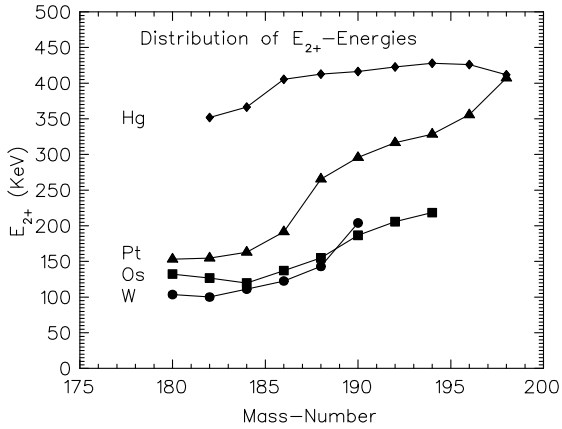

Figure 14: 2^+ level-energies versus mass number of W, Os, Pt and Hg.

γ-unstable. The proposed level scheme of ^{190}W fits consistently with the level-energy systematics of the lighter W-isotopes. If one normalizes the level energies to the 2^+ energy one observes (Fig.13) a strong deviation from the I·(I+1) law for light and heavy W isotopes. The deviation at the neutron rich side is quite dramatic. For the 6^+ and the 8^+ gs-levels of ^{188}W energies are taken from [8] although the spins of these levels are still not definitely assigned. If one compares the behaviour of the first excited 2^+ states with other isotopic chains (Fig.14), one notes a sharp increase of the energy of W on the n-rich side, which is more gradual for the Os-isotopes but comparable with the Pt-chain.

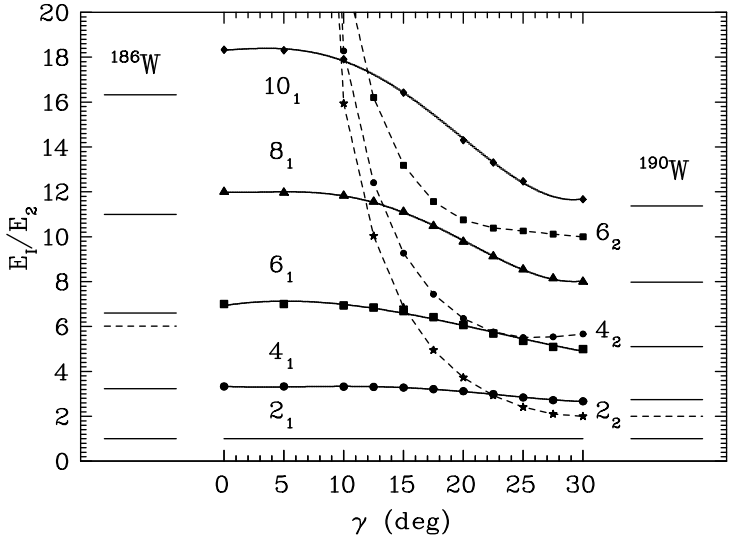

Figure 15: Normalized gs-level energies as a function of the triaxial deformation parameter γ in comparison with the level schemes of ^{186}W and ^{190}W.

Using the triaxial rotor model one can see (Fig.15) that ^{190}W shows the behaviour of a γ-deformed rotor. The normalized level energies are compatible with a γ of 30°. In contrast, ^{186}W has a weak triaxial deformation ($\gamma \approx 15°$).
If one takes also the value of the second 2^+' state and the transition 4^+'$\rightarrow 2^+$' from the calculation one can find corresponding small peaks in the γ-ray spectrum of ^{190}W, supporting the present interpretation.

This work was supported by GSI, EPSRC(UK), CEA/DSM/DAPNIA (France), the EU Access to Large Scale Facilities Program and the Polish Committee of Scientific Research under grant KBN 2 P03B 036 15.

References

[1] K. Jain et al. Nucl. Phys. **A591** (1995) 61
[2] C.S. Purry et al. Nucl. Phys. **A632** (1998) 229
[3] P.M. Walker et al. Phys. Lett. **B408** (1997) 42
[4] G.D. Dracoulis et al. Phys. Rev. **C58** Vol. 3 (1998) 1444
[5] N. Kanako et al., Nucl. Phys. **A601** (1996) 69
[6] M. de Jong et al., Nucl. Phys. **A613** (1997) 435
[7] H.G. Clerc et al., Nucl. Phys. **A538** (1992) 367c
[8] R.B. Firestone, Table of Isotopes, John Wiley & Sons, Inc. (1996)
[9] H. Geissel et al., Nucl. Instr. and Meth. **B 70** (1992) 286
[10] M. Pfützner et al., Phys. Lett. **B444** (1998) 32
[11] P.M. Walker et al., Nucl. Phys. **A568** (1994) 397
[12] e.g. P. Reiter et al., Phys. Rev. Lett. **82** (1999) 509